

Comparison of Basic Linear Filters in Extracting Auditory Evoked Potentials

Serap AYDIN

*University of Ondokuz Mayıs, Faculty of Engineering, Electrical and Electronics
Engineering Department, Kurupelit Campus, 55139 Samsun-TURKEY
e-mail: drserapaydin@hotmail.com*

Abstract

In the present study, the performances of two well-known linear filtering techniques are compared for extraction of auditory Evoked Potential (EP) from a relatively small number of sweeps. Both experimental and simulated data are filtered by the two algorithms into two groups. Group A consists of Wiener filtering (WF) applications, where conventional WF and Coherence Weighted WF (CWWF)) have been assessed in combination with the Subspace Method (SM). Group B consists of the well-known adaptive filtering algorithms Least Mean Square (LMS), Recursive Least Square (RLS), and one-step Kalman filtering (KF). Both groups are tested with respect to signal-to-noise ratio (SNR) enhancement by comparing to the traditional ensemble averaging (EA). We observed that KF is the best method among them. The application of the SM before filtering improves the performance of the LMS and the assessments of WF where the CWWF works better than the conventional WF in that case.

In conclusion, most of the linear filters show definitely better performance compared to EA. KF effectively reduces the experimental time (to one-fourth of that required by EA). The SM that has recently been revealed in EP estimation is found to be a meaningful pre-filter as it significantly reduces the noise level of EEG raw data.

Key Words: *Adaptive filtering, Wiener filtering, auditory evoked potential, EEG.*

1. Introduction

Recordable brain electrical signals due to external stimuli are called Evoked Potential (EPs), or event-related potentials (ERPs). Since these weak signals are buried in signals of spontaneous electroencephalogram (EEG) with very low signal-to-noise ratio (SNR), large numbers of repetitions are ensemble-averaged (EA) to recognize them. However, the time-locked EP signal and stimulus independent background EEG noise are assumed to be uncorrelated in this traditional technique. With this assumption in mind, there are also works which discuss the reliability of EA considering the possible EP component variability depending on the psycho-physiological factors for a given individual [16]. Thus, many researchers have focused on the ensemble reduction in extracting a template EP, assuming the stimulus-induced changes in the EEG are small [1–4, 7, 12, 13, 16].

Template EP signals are important clinical tools in diagnoses. However, where there are relatively

tight constraints related to the available recording time or cooperation of the subject, collection of large adequate sweeps is impractical. This has led to development of alternative methods to improve SNR based on the additive model. Some of these algorithms involve weighted averaging [7], adaptive filtering [12], Wiener filtering [13], and transform-based algorithms [1–4]. The purpose of this study is to compare the performance of ordinary Wiener filtering approaches and well-known adaptive filtering algorithms in the extraction of the template auditory EPs from a relatively small number of sweeps.

To reduce the number of sweeps needed to obtain an EP with adequate SNR, various estimation techniques such as least squares (LS), mean square, or Bayesian are being used as either an alternative to EA or a post-processing step to remove the remaining noise on the average signal. Recursive least squares (RLS), one-step Kalman filtering (KF) and Subspace Method (SM) are basic LS sense estimation methods. The SM, i.e. an orthogonal projection approach based on singular value decomposition, is usually proposed to filter noisy image components in image processing [18]. In the present study, we have applied this linear algorithm to actual brain EP measurements to reduce the EEG noise level without loss of information before the secondary filtering algorithms of conventional WF, Coherence Weighted WF (CWWF) [13], and LMS filtering.

In the second main part of our study, the LMS, RLS and KF can be classified as adaptive algorithms and their performance should be studied separately. We compare them with conventional EA for various kinds of experimental data sets where the KF was found to be favorable among the other ones [1–3]. In literature, the LMS algorithm is frequently used in various adaptive filtering approaches to extract the template EP due to its computational simplicity [12] whereas the algorithms of RLS and KF were rarely chosen to estimate the parameters of adaptive noise canceling algorithms. However, the main drawback of the LMS algorithm is the slow convergence speed that depends inversely on the eigenvalue spread of the input correlation matrix for a fixed step size. Any slight change in the step size affects the stability in convergence. The sensitivity of the estimation on step-size was highly diminished by using time domain moving windows [15].

In EP research, adaptive algorithms are also used to model EPs based on LMS filtering [19], and KF [17]. We tested the one-step adaptive KF algorithm in our former work in comparison to the RLS and the LMS [2, 3]. These basic adaptive algorithms form the second group in this assessment.

All methods in both groups, are implemented with the following three assumptions: 1) the EP signal is stationary; 2) the EP and background EEG noise are uncorrelated; and 3) the background EEG noise is independent of the stimulus. Thus we adopt the well-known additive signal model to perform the linear filtering algorithms for auditory brain activities. Theoretical basis and related definitions are briefly introduced in Section 2. We give results in association with simulations and experimental studies, as well as pseudo-simulations, in Section 3.

2. Methods

The EP signal s and the ongoing EEG sequence z are assumed to be additive in consecutive noisy measurements x . Mathematically, this basic assumption is expressed by an additive signal model in the form

$$x_i(n) = s(n) + z_i(n). \quad (1)$$

Here, n is the time index and i denotes the trial number, where $n = 1, \dots, N$, $i = 1, \dots, L$. For empirical data, the grand average is taken as the template EP:

$$x_{\text{ga}} = \sum_{i=1}^M x_i(n), \quad M \geq 512, M \gg L. \quad (2)$$

The aim of this study is to estimate the clear EP from L number of records instead of M . For that purpose, noisy measurements to be filtered is formed by replacing the sweeps into separate columns of a matrix:

$$\mathbf{X} = \begin{bmatrix} x_1(1) & x_2(1) & \cdots & x_L(1) \\ x_1(2) & x_2(2) & \cdots & x_L(2) \\ \vdots & \vdots & & \vdots \\ x_1(N) & x_2(N) & \cdots & x_L(N) \end{bmatrix} = \begin{bmatrix} s(1) & s(1) & \cdots & s(1) \\ s(2) & s(2) & \cdots & s(2) \\ \vdots & \vdots & & \vdots \\ s(N) & s(N) & \cdots & s(N) \end{bmatrix} + \begin{bmatrix} z_1(1) & z_2(1) & \cdots & z_L(1) \\ z_1(2) & z_2(2) & \cdots & z_L(2) \\ \vdots & \vdots & & \vdots \\ z_1(N) & z_2(N) & \cdots & z_L(N) \end{bmatrix}.$$

Then, one can write the raw data in matrix form as

$$\mathbf{X} = \mathbf{S} + \mathbf{Z}. \quad (3)$$

The signal matrix \mathbf{S} is estimated by linear filtering algorithms in the present work. The related methods are briefly presented in the following sections.

2.1. Group A: Wiener Filtering Approach

The conventional Wiener Filter (WF) and the Coherence Weighted WF (CWWF) are applied to the projected version of the raw data. The combination order of the methods is also changed. The algorithms used are denoted with the names below:

- 1) WFSM: The filtered data is projected in least-square sense.
- 2) SMWF: The projected version of the observations is filtered by the WF.
- 3) SMCWWF: The projected version of the observations is filtered by the CWWF.

Theoretical definitions for each method are given in the following sub-sections.

2.1.1. The Subspace Method



Figure 1. Block diagram of the SM application

The SM linearly projects the raw data in a least-square sense. The resulting output matrix is denoted by R , given in Figure 1. The SM assumes that the stationary EP is modeled by linear combination of some basis functions in the form

$$s = H\theta = \sum_{i=1}^r h_i \theta. \quad (4)$$

Here, scalar unknown parameters of θ are real multipliers of the basis vectors of h_i . Then the model parameters are estimated into least-square sense estimation though the relations

$$J(\theta) = (x - H\theta)^T (x - H\theta)$$

$$\frac{\partial J(\theta)}{\partial \theta} = 0 \Rightarrow \hat{\theta} = (H^T H)^{-1} H^T x, \tag{5}$$

where $J(\theta)$ denotes the Jacobian form of unknown parameter vector, θ . Then, single signal vector is estimated by substituting equation (5) into equation (4), obtaining

$$\hat{s} = H\hat{\theta} = H (H^T H)^{-1} H^T x, \tag{6}$$

where the model matrix can be chosen as Gaussian shaped functions having a smooth waveform similar to the EP. Matrix multiplication $H (H^T H)^{-1} H^T$ is called the projection matrix in the literature [10]. So, considering a matrix form in equation (3), the approximate signal matrix can be written as

$$\hat{S} = H (H^T H)^{-1} H^T X, \tag{7}$$

where the number of model matrix's columns refers to the signal subspace dimension. In other words, EP approximations lie in r -dimensional subspace, if the r -numbers of basis is linearly independent. When, a small number of noisy observations are considered as a real-valued noisy matrix that is summation of clear signal matrix and uncorrelated noise matrix as formulated in equation (3), the dominant left eigenvectors of X can be chosen as linear independent basis vectors [11]. So, the projected version of X can be written in the form

$$R = U^T (U U^T)^{-1} U X = U^T U X, \tag{8}$$

where the matrix U is computed from singular-value-decomposition pairs of X such that

$$\text{svd}(X) = [U \quad \bar{U}] \text{diag}(\sigma_1, \sigma_2, \dots, \sigma_L) \begin{bmatrix} V \\ \bar{V} \end{bmatrix}. \tag{9}$$

Note there is a gap between the eigenvalues $(\sigma_r) \gg (\sigma_{r+1})$, if $\text{rank}(X) = r$.

2.1.2. Wiener Filtering Algorithms

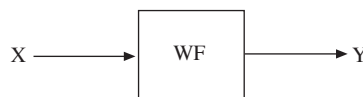


Figure 2. Block diagram of the WF applications.

Elementary properties of the WF is summarized by the block diagram shown of Figure 2 [8].

Let noisy sweep $x_i(n)$ be filtered. Then the desired signal is computed by the relation

$$d_i(n) = \frac{1}{L-1} \sum_{j=1, j \neq i}^L x_j(n). \tag{10}$$

The corresponding filter output sequence $y_i(n)$ is computed as

$$y_i(n) = \sum_{m=0}^{N-1} h_i(m) x_i(n-m), \tag{11}$$

where $h_i(n)$ refers to the filter impulse response (that is the solution of Wiener-Hopf equations) in the form

$$p_i(-k) = \sum_{m=0}^{N-1} h_i(m)r_{x_i}(m-k), \quad k = 0, \dots, M-1, \quad (12)$$

Here r_{x_i} is the autocorrelation vector of the input noisy sweep and p_i is the cross-correlation function between the input signal and the desired signal. For a stationary signal, the filter coefficients are estimated by

$$h_i = R_{x_i}^{-1}p_i. \quad (13)$$

The filter impulse response can be also computed in an iterative way to account for the EEG power variations in the CWWF [13]. Then, the filter transfer function is computed from the relations

$$H(w) = \frac{S_s(w)}{S_s(w) + \frac{S_x(w)}{L-1}} \quad (14)$$

$$S_s(w) = \frac{L}{L-1}S_{\bar{x}}(w) - \frac{1}{L-1}S_x(w). \quad (15)$$

The power spectral densities $S_s(w)$, $S_x(w)$ and $S_{\bar{x}}(w)$ are squared magnitude of the Fourier Transform of the signal s , noisy sequence \mathbf{x} and an average sequence $\bar{\mathbf{x}}$, respectively. These spectra are calculated iteratively. The coherence function γ_{xz} , which reflects the degree of correlation between the different frequency components of two stationary time sequences x and z is calculated as

$$\gamma_{xz} = \frac{S_{xz}(w)}{\sqrt{S_{xx}(w)S_{zz}(w)}}. \quad (16)$$

Then, the filter transfer function is obtained in the form

$$H(w, i) = \frac{S_s(w, i)}{S_s(w, i) + \frac{S_x(w, i)}{L-1}}, \quad (17)$$

where the inverse transform this function gives the impulse response of the filter [13].

2.2. Group B: LMS, RLS and KF Approaches



Figure 3. Block diagram of the AF applications.

LMS, RLS algorithms and KF are linear adaptive filtering algorithms, performed as introduced in literature [8] with respect to the block diagram shown in Figure 3.

The filter output denoted by $y_i(n)$ is computed by,

$$y_i(n) = x_i(n) * w_i(n). \quad (18)$$

Here, $w_i(n)$ refers the estimated filter coefficients, where $*$ denotes linear convolution. The target of the AF, namely the desired signal, $d_i(n)$, is calculated from the average of L sweeps, excluding the input sequence of interest, as

$$d_i(n) = \frac{1}{L-1} \sum_{j=1, j \neq i}^L x_j(n). \quad (19)$$

Thus, the estimation error is $e_i(n) = d_i(n) - y_i(n)$. The error is minimized by different estimation techniques into AF applications. In case of the LMS (a stochastic gradient search algorithm), the error is minimized in mean-square sense. Mathematically, it is expressed by $J(n) = E \{ |e(n)|^2 \}$. This is realized by moving along the negative gradient direction with a step-size of μ . The related filtering algorithm can be summarized using the following formula:

$$\hat{w}_i(n+1) = \hat{w}_i(n) + \mu x_i(n) e_i^*(n), \quad (20)$$

where $\hat{w}_i(n)$ is the tap-weight vector whose entries are initially equal to zero.

In case of the RLS algorithm, the least-square sense estimation is assessed such that the tap-weight vector, consisting of the filter coefficients, is estimated by minimizing the exponentially weighted least-squared error expressed by $J(n) = \sum_{i=1}^N \lambda^{n-i} |e_i(n)|^2$. Then, the filter coefficients are estimated by using the update equation in form

$$\hat{w}_i(n) = \hat{w}_i(n-1) + k_i(n) e_i^*(n), \quad (21)$$

$$k_i(n) = \frac{P_i(n-1) x_i(n)}{\lambda + x_i^H(n) P_i(n-1) x_i(n)}, \quad (22)$$

$$P_i(n) = \lambda^{-1} P_i(n-1) - \lambda^{-1} k_i(n) x_i^H(n) P_i(n-1), \quad (23)$$

where λ is the exponential memory weighting factor and $P_i(n)$ is the input correlation matrix having an initial setting as given by $P_i(n) = \delta^{-1} I$. The RLS algorithm is a special case of the KF. The KF solves the recursive minimum least-square sense estimation problem based on the state-space concept. In one-step adaptive KF algorithm, the tap-weight adaptation is computed as

$$\hat{w}_i(n+1) = \hat{w}_i(n) + g_i(n) e_i^*(n), \quad (24)$$

$$g_i(n) = \frac{K_i(n-1) x_i(n)}{Q_m + x_i^H(n) K_i(n-1) x_i(n)} \quad (25)$$

where $g_i(n)$ denotes the Kalman gain. KF leads to minimization of the trace of the filtered state error correlation matrix $K_i(n)$, which is calculated as

$$K_i(n) = K_i(n-1) - g_i(n) \hat{x}(n) K_i(n-1) + Q_p. \quad (26)$$

Here, Q_p and Q_m are the autocorrelation matrices associated with the measurement noise sequence and the process noise sequence, respectively. These noise vectors are assumed uncorrelated white noise processes. The initial setting of the KF algorithm is given by $K_i(0) = k_0 I$.

The adaptive filtering algorithms used above filter not only raw data but also the projected version of the data. The SM does not provide notable benefits for both RLS and KF whereas the performance of LMS algorithm is remarkably increased.

3. Results

3.1. Data Collection

Experimental data was recorded from the left mastoid of eight subjects listening to binaurally delivered stimuli via headphones. Vertex electrode was used as the reference. The pass-band of the amplifier was 0.3–70 Hz and the amplifier noise was 2 μ V. During the experiments, the subject was sitting on a chair in an electrically and acoustically shielded room. The stimuli were 1 kHz tones of 100 ms duration and 80 dB Hearing Level intensity, presented with an inter stimulus interval of 2 sec. 512 single sweeps were acquired with a sampling rate of 250 samples/sec. The epoch length was 1 sec, including a 200 ms pre-stimulus part. The SNR of a single sweep (with respect to the grand average of 512 sweeps) was found to be about -5 dB.

3.2. Simulations

In pseudo-simulations, actual spontaneous EEG measurements collected from the volunteers without any stimulation were added to the generated EP.

In simulations, ensemble average of 1200 actual auditory single epochs collected from healthy volunteers is assumed to be a template EP. To these auditory epochs white noise sequences were added to the known EP for several generated noise variance cases. The generated data sets having 40 sweeps with a specific SNR are mentioned as simulations in the present study.

3.3. Results for Group A

Figure 4 and Figure 5 show changes in the output SNR values for different number of sweeps used in simulations and pseudo-simulations, respectively. In simulations, the SMCWWF provides superior results compared to EA. WF, WFSM and SMWF provide only marginal improvement.

In pseudo-simulations, the WF does not provide SNR improvements. For 40 sweeps, the SMCWWF provides 45 dB of output SNR. For the first 20 sweeps, Group A does not have good performance. For more sweeps, both the SMWF and SMCWWF provide more SNR enhancement compared to the EA. Figure 6 shows the estimated waveforms for 20 sweeps having -5 dB of SNR. Figure 7a shows the output SNR values versus the number of experimental sweeps. Both SMWF and SMCWWF provide higher SNR improvements compared to EA. The waveforms of the estimations for 64 sweeps are given in Figure 7b. There are undesired noise fluctuations in both pre-stimulus and post-stimulus intervals. The main positive and negative peaks of the grand average are obtained without distortion by using the SMCWWF and SMWF.

To find the maximum SNR that a method can achieve in the experimental studies, the number of sweeps is increased from 32 to 511 (the average of 512 sweeps is considered as the AEP signal). The ensemble average yields an SNR of 68 dB for 511 sweeps and the methods of SMCWWF and SMWF reach to this value when only 128 sweeps are used. Beyond 128 sweeps, no further improvements are observed. When the WFSM is used, the output SNR increases to 45 dB when 100 sweeps are used and remains constant even the number of sweeps is more than 100.

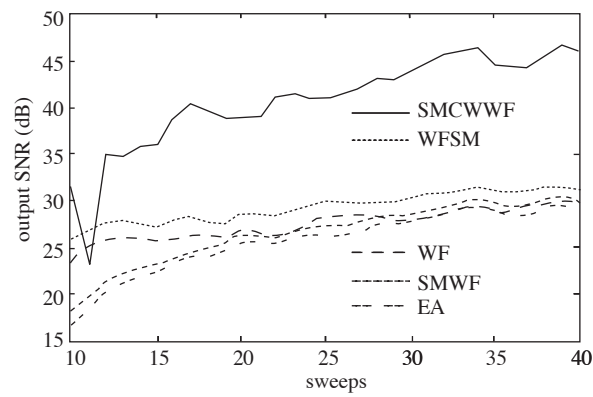


Figure 4. Output SNR improvements of Group A versus the number of simulated sweeps.

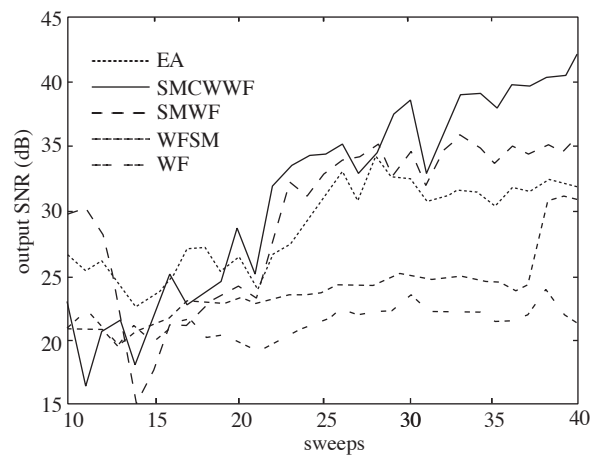


Figure 5. Output SNR improvements of Group A versus the number of pseudo-simulated sweeps.

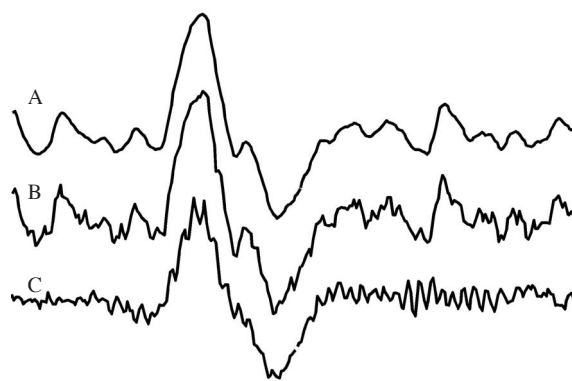


Figure 6. The waveforms of the estimations in simulations where A, B and C refer to SMCWWF, SMWF and WFSM, respectively.

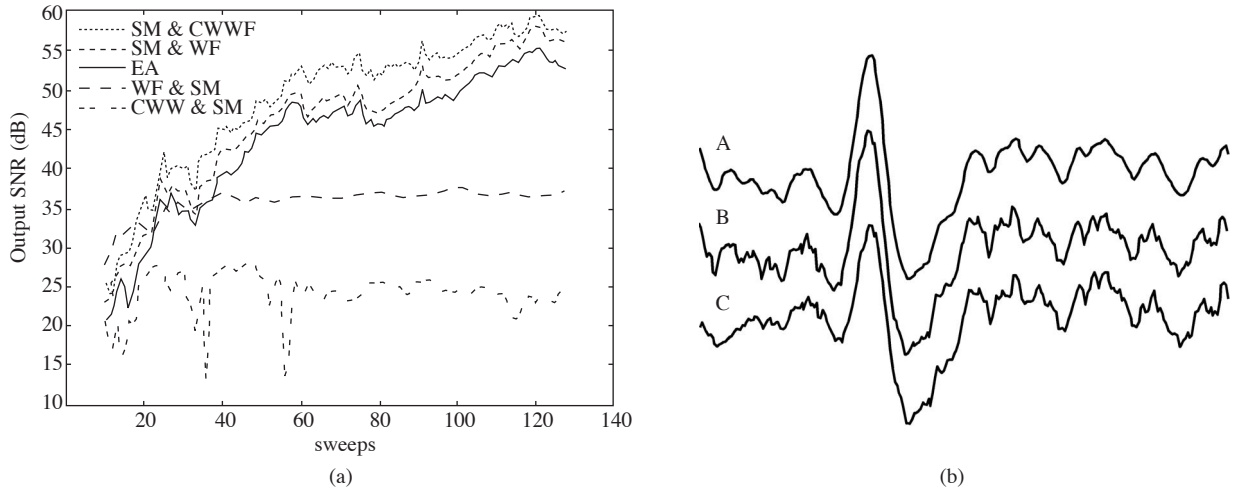


Figure 7. a) The output SNR improvements of Group A versus the number of actual sweeps. b) The waveforms of the estimations for 64 sweeps, where A, B and C refer to SMCWWF, SMWF and WFSM, respectively.

3.4. Results for Group B

The optimal filter parameters are chosen empirically for actual data collected from eight healthy volunteers, as

$$\mu = 0.000011, \quad \lambda = 0.001, \quad \delta = 0.1, \quad q_p = 100, \quad q_m = 0.1, \quad k_o = 0.2.$$

A filter length $M = 50$ is found to be appropriate for all actual data sets. Note that the adjusted parameter values may change depending on variations of stimulus type and experimental conditions.

Figure 8 and Figure 9 show changes in the output SNR values for different number of sweeps in simulations and pseudo-simulations, respectively. In simulations, three algorithms in Group B provide better SNR improvements when compared to the EA. When 10 sweeps are used, an SNR enhancement of 16 dB is obtained by using the RLS filtering. This high performance is preserved as the number of sweeps is increased. When 40 sweeps are used, it is possible to obtain an output SNR of 47 dB using the RLS filtering. However, the output SNR can only reach 28 dB with the EA. In pseudo-simulations, the RLS provides an improvement of 5 dB above that of the EA. The LMS filtering is found unsuccessful. When the LMS filter is applied to the projections, the output SNR improves, yet it remains below the corresponding values provided by the EA. The number of sweeps to be projected also affects the filtering performance. Thus, increasing sweep number to 32 improves the performance notably. The related waveforms of the estimations are shown in Figure 9.

For both studies, the clearest waveforms are obtained by using the RLS and KF. Figure 10 shows changes in the output SNR values for incremental number of actual sweeps. The KF appears to have the best performance. When more than 20 sweeps are filtered, KF provides an SNR enhancement of 15 dB above EA. The related waveforms of estimations are shown in Figure 11, where 64 single epoches are filtered. KF provides the highest SNR improvement. RLS filtering and the SMLMS method show nearly the same performance.

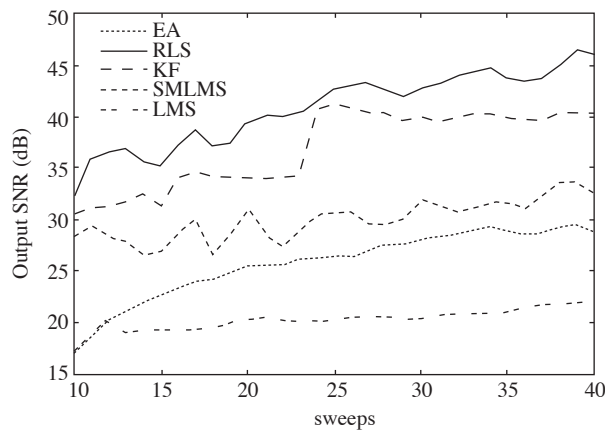


Figure 8. Output SNR improvements of Group B versus the number of simulations.

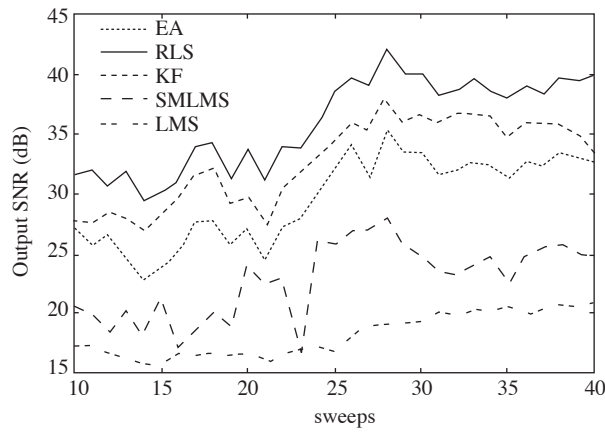


Figure 9. The output SNR improvements of Group B versus the number of pseudo-simulations.

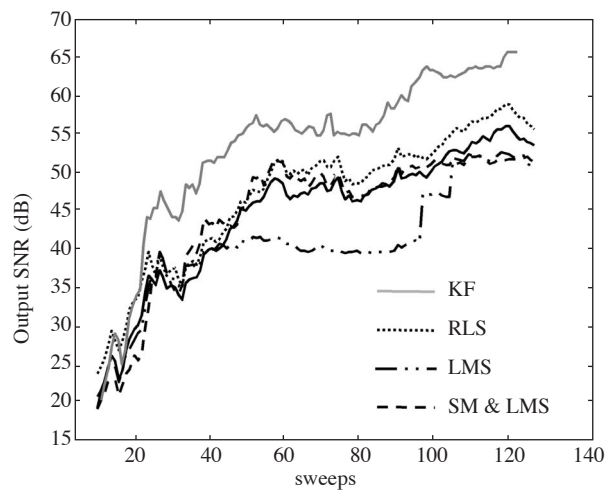


Figure 10. The output SNR improvements of Group B versus the number of actual sweeps.

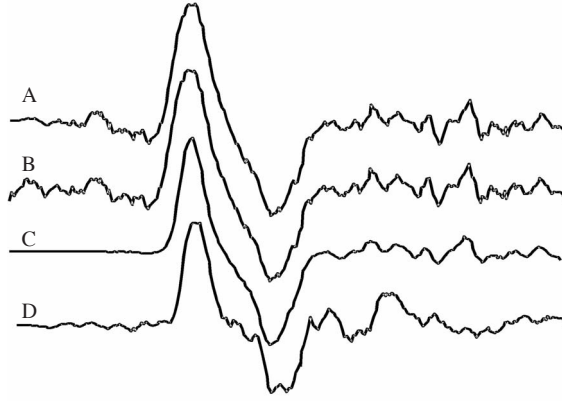


Figure 11. The waveforms of the estimations of simulations where A, B, C and D refer to RLS filtering, KF, SMLMS and LMS filtering, respectively.

3.5. Computational Complexity

Computational complexity (CC) of the discussed algorithms is investigated from various sources [3, 5]. The corresponding measures are shown in Table 1. Thus, it can be said that the LMS filtering is the least computationally complex. However, the LMS is found to be unsuccessful if it is not combined with the SM in our comparison work. The CC of the KF, having the best performance among all algorithms, is adequate. The combination of the SM and the CWWF requires memory of $NL^2 + (N\text{Log}_2^N)/2$ such that this value is high.

Table 1. Computational Complexity properties of the algorithms.

	SM	WF	CWWF	LMS	RLS and KF
CC	NL^2	M^2	$(N\text{Log}_2^N)/2$	M	M^2

4. Conclusions

The results show that, the SM can remove a large amount of EEG noise. In addition, the characteristic of the EEG noise remaining on the projections renders white noise. Thus, the SMCWWF was found to be better than the SMWF for all data sets. Thus CWWF is the better alternative to the WF in spite of its higher computational complexity.

In the Group B, the RLS and KF were better compared to EA. The RLS is the best filter in simulations, whereas the KF provides the highest performance in experimental studies. When we analyze the KF after 128 sweeps, it shows characteristic of a low-pass filter, which has a narrower bandwidth, compared to the RLS filter, indicating the possibility of better performance.

The LMS filter performance depends on 1) the number of sweeps, 2) the step size parameter, 3) the filter length, and 4) the input SNR of single sweeps. It was, in general, found unsuccessful for low input SNR cases. The selection of step size parameter was assumed to be the crucial factor in the performance. To obtain a better performance with the LMS filtering, various methods were proposed which explore an optimum step-size at each iteration [8]. In another study, the optimum value was determined methodologically considering the filter length, input signal variance and the desired signal [2]. In the present study, these approaches

are not attempted; instead the performance of the SMLMS algorithm is tested. The SMLMS algorithm appeared to be relatively less sensitive to the step size and showed better performance compared to the EA in both experimental and simulation trials. However, its performance in the pseudo-simulations proves again unsatisfactory. In conclusion, we leave the following matters for future work: 1) the use of optimal step size, and, 2) exploring further properties of the SMLMS algorithm for better performance.

In conclusion, most of the basic linear estimation techniques show definitely better performance than EA in extracting the EPs. The KF effectively reduce the experimental time (to one-fourth of that required by EA). The SM proves to be a useful pre-EEG filter.

Acknowledgement

We wish to thank Prof. Dr. Pekcan Urgan of Hacettepe University for providing the experimental data sets.

References

- [1] S. Aydın, *Extraction of auditory evoked potentials from ongoing EEG*, METU, Ankara, 2005.
- [2] S. (Aydın) Kılıç, G. Gençer and B. Baykal, *Comparison of algorithms in extracting of auditory evoked potentials*, IEEE The 23rd Conf on EMBS, Cancun, 2003.
- [3] S. Aydın, *Basic Linear Filters in Extracting of Auditory Evoked Potentials*, IEEE Int Symposium on Signal Processing and Analysis, İstanbul, Turkey, 2007.
- [4] S. Aydın, *An Assessment of Tikhonov Regularizations to Evoked Brain Signals*, IEEE Int Symposium on Signal Processing and Analysis, İstanbul, Turkey, 2007.
- [5] R. Y. Chen, C. L. Wang, "On the optimum step size for the adaptive sign and LMS algorithms", *Trans on Circuits and Systems*, IEEE, 37(6), 1990, pp.836–840.
- [6] T. H. Cormen, C. E. Leiserson, *Introduction to Algorithms*, MIT Press, 1990.
- [7] C. E. Davila and R. Srebro, "Subspace averaging of steady-state visual evoked potentials", *Trans on BME*, IEEE, 37(6), 2000, pp.720–728.
- [8] S. Haykin, *Adaptive Filter Theory*, Prentice Hall, 1991.
- [9] P. A. Karjalainen, J. P. Kaipio, "Subspace regularization method for the single-trial estimation of evoked potential", *Trans on BME*, IEEE, 46, 1999, pp. 849-859.
- [10] S. Kay, *Fundamentals of statistical signal processing*, Prentice Hall, 1993.
- [11] V. Klema, A. Laub, "The singular value decomposition: Its computation and some applications", *Trans on Auto Cont*, IEEE, 25(2), 1980, pp. 164–176.
- [12] R. H. Kwon, G., E.W. Johnston, "A variable step size LMS algorithm", *Trans on Sig.Proc.*, IEEE, 40(7), 1992, pp. 1633-1642.
- [13] P. Laguna, R. Jane, "Adaptive Filter for event-related bioelectric signals using an impulse correlated reference input", *Trans on BME*, IEEE, 39, 1992, pp. 1032-1043.

- [14] J. S. Paul, A. R. Luft, D. F. Hanley and N. V. Thakor, “Coherence-Weighted Wiener filtering of somatosensory EPs”, *Trans on BME*, IEEE, 48, 2001, pp. 1483–1488.
- [15] J. Tian, M. Juhola,, “Latency estimation of auditory brainstem response by neural networks”, *Artif. Intel. In Med.*, Elsevier, 10(2), 1997, pp. 115–128.
- [16] W. Qiu, S.M. Fung, H.Y. Chan, “Adaptive filtering of evoked potentials with radial basis function neural network pre-filter”, *Trans on BME*, IEEE, 49, 2002, pp. 225–231.
- [17] T. W. Picto, *Handbook of EEG and Clinical Neurophysiology*, Elsevier Series, 1989.
- [18] M. V. Spreckelsen and B. Bromm., “Estimation of single-evoked cerebral potentials by means of parametric modeling and Kalman filtering”, *Trans on BME*, IEEE, 35, 1988, pp. 691–699.
- [19] H. Ren, C. Chang, “A generalized orthogonal subspace projection approach to unsupervised multi-spectral image classification”, *Trans on Geoscience.*, IEEE, 38, 2000, pp. 2515–2528.
- [20] C. A. Vaz and N. V. Thakor, “Adaptive Fourier estimation of time-varying EPs”, *Trans on BME.*, IEEE, 4, 1989, pp. 448–455.